HHS Public Access

Author manuscript

Stem Cells. Author manuscript; available in PMC 2019 April 01.

Published in final edited form as:

Stem Cells. 2018 April ; 36(4): 616–625. doi:10.1002/stem.2752.

Alpha-Klotho Enrichment in Induced Pluripotent Stem Cell Secretome Contributes to Antioxidative Protection in Acute Lung Injury

Amiq Gazdhar[1,2,*], **Priya Ravikumar**[3,4,*], **Johanne Pastor**[4], **Manfred Heller**[2], **Jianfeng Ye**[4], **Jianning Zhang**[3,4], **Orson W. Moe**[3,4,5], **Thomas Geiser**[1,2], and **Connie C.W. Hsia**[3,†]

[1]Dept. of Pulmonary Medicine, University Hospital, Bern, Switzerland [2]Dept. of Clinical Research, University Hospital, Bern, Switzerland [3]Dept. of Internal Medicine, University of Texas Southwestern Medical Center, Dallas, TX, USA [4]Charles & Jane Pak Center of Mineral Metabolism & Clinical Research, University of Texas Southwestern Medical Center, Dallas, TX, USA [5]Dept. of Physiology, University of Texas Southwestern Medical Center, Dallas, TX, USA

Abstract

Induced pluripotent stem cells (iPSCs) has been reported to alleviate organ injury, although the mechanisms of action remain unclear and administration of intact cells faces many limitations. We hypothesized that cell-free conditioned media (CM) containing the secretome of iPSCs possess antioxidative constituents that can alleviate pulmonary oxidant stress damage. We derived iPSCs from human dermal fibroblasts and harvested the CM. Addition of iPSC CM to cultured human alveolar type-1 epithelial cells mitigated hyperoxia-induced depletion of endogenous total antioxidant capacity (TAC) while tracheal instillation of iPSC CM into adult rat lungs enhanced hyperoxia-induced increase in TAC. In both the in vitro and in vivo models, iPSC CM ameliorated oxidative damage to DNA, lipid and protein, and activated the nuclear factor (erythroid-derived 2)-like 2 (Nrf2) network of endogenous antioxidant proteins. Compared to control fibroblast-conditioned or cell-free media, iPSC CM is highly enriched with αKlotho at a concentration up to more than 10-fold of that in normal serum. αKlotho is an essential antioxidative cell maintenance and protective factor and an activator of the Nrf2 network. Immunodepletion of αKlotho reduced iPSC CM-mediated cytoprotection by ~50%. Thus, the abundant αKlotho content significantly contributes to iPSC-mediated antioxidation and cytoprotection. Results uncover a major mechanism of iPSC action, suggest a fundamental role of αKlotho in iPSC maintenance, and support the translational potential of airway delivery of cell-free iPSC secretome for protection against lung injury. The targeted cell-free secretome-based approach may also be applicable to the amelioration of injury in other organs.

[†]**Correspondence author:** Connie C.W. Hsia, M.D., Dept. of Internal Medicine, University of Texas Southwestern Medical Center, 5323 Harry Hines Blvd., Dallas, TX 75390-9034, TEL: 214-648-3426, Connie.Hsia@utsouthwestern.edu.

[*]Equal contribution

Disclosure of Potential Conflict of Interest

Thomas Geiser declared Advisory role with Boehringer Ingelheim, Novartis, and Roche. Dr. Geiser also received Honoraria for speaking fees from Novartis, BI, and Roche.

All other authors have declared no conflict of interest.

Legend of Graphical Abstract

The secretome of human induced pluripotent stem cells (iPSCs) contains abundant αKlotho, an antioxidative cytoprotective protein that activates Nrf2-responsive genes, increases total antioxidant capacity and alleviates oxidative damage in vitro and in vivo. Immunodepletion of αKlotho significantly impairs iPSC secretome-mediated cytoprotection from hyperoxia-induced damage.

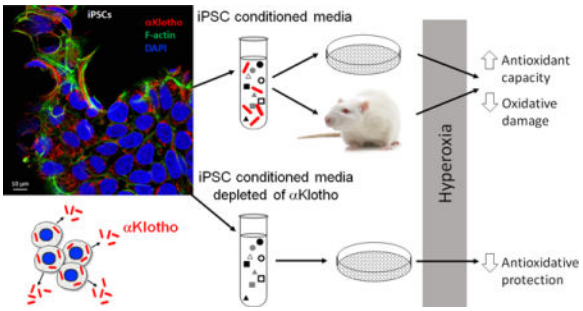

Keywords

iPS cells; stem cells; secretome; acute lung injury; hyperoxia; oxidative stress damage

Introduction

Induced pluripotent stem cells (iPSCs) can re-differentiate into various mature cell types and expand in large numbers to be given as patient-specific autologous therapy. Preclinical studies have shown the efficacy of iPSCs in alleviating injury from physical, infectious, ischemic, chemical and metabolic insults in various tissues [1–5]. Direct iPSC administration *in vivo* is limited by a low cell engraftment rate and undesired off-target effects [6] including immunogenicity [7, 8], non-specific differentiation, and tumor transformation [9]. One alternative is administration of cell-conditioned media (CM) containing the secreted products of iPSCs, which could induce similar biological responses as intact cells and with fewer adverse effects. Gazdhar et al. [10] reported that iPSCs derived from human fibroblasts facilitated alveolar epithelial wound repair *in vitro* while tracheal instillation of iPSC secretome reduced expression of collagen and profibrotic mediators in bleomycin-induced pulmonary fibrosis. The mechanisms of action of iPSC secretome remain poorly understood. Hepatocyte growth factor (HGF) [10] and interferon-γ induced protein 10 [5, 11] have been detected in iPSC secretome and postulated to participate in repair and regeneration. Owing to the complex components of iPSC secretome, interactive modulation of multiple mediators and homeostatic pathways likely plays a major role in promoting beneficial outcome at cellular and organ levels.

A common feature of tissue injury is heightened oxidative stress that outstrips endogenous antioxidant capacity, leading to redox imbalance and tissue damage. We hypothesized that iPSCs secrete potent antioxidants to protect from tissue injury. As lung cells are uniquely susceptible to oxidant injury and the intact lung is readily accessible to targeted delivery of therapeutic agents, we tested the ability of iPSC secretome to protect lung cells *in vitro* and

lungs *in vivo*. Our results established the ability of iPSC secretome to activate endogenous antioxidant genes in the nuclear factor (erythroid 2)-related factor 2 (Nrf2) network to alleviate oxidative damage *in vitro* and *in vivo*. We identified that iPSCs produce abundant αKlotho, a potent antioxidative cytoprotective factor that activates the antioxidant response element (ARE) of Nrf2 target genes, and showed that αKlotho enrichment contributes significantly to iPSC secretome-mediated cytoprotection.

Materials and Methods

Study design

Our objective was to test whether iPSC secretome alleviates oxidative damage and uncover the underlying mechanisms. The lung served as a target organ owing to its susceptibility to diffuse oxidant injury [12, 13] and ease of access. Airway delivery of test agents to the lung also minimizes systemic off-target effects. The protocols were approved by the UT Southwestern Institutional Animal Care and Use Committee and followed the National Institutes of Health Guide for the Care and Use of Laboratory Animals.

Generation of iPSCs secretome

iPSCs were generated from human foreskin fibroblasts (CRL-2429; American Type Culture Collection (ATCC), Rockville, MD) following established procedure [14]. The CHiPS-W iPSCs that had been fully characterized in vitro and in vivo by Grad et al [14] were used in this study. Briefly, after expansion 5×10^4 human fibroblasts were infected with multiplicity of infection of 5 pSin-EF2-Nanog-Pur, treated with puromycin × 5 d, then retransduced with 3 viruses: pSin-EF2-Sox2-Pur, pSin-EF2-Oct4-Pur and pSin-EF2-Lin28-Pur (multiplicity of infection 5). iPSCs were maintained on irradiated human foreskin fibroblasts (CCD1; ATCC) in knockout Dulbecco's modified Eagle's medium (DMEM) supplemented with 20% serum replacement, 2 mmol/l Glutamax, 40 μg/ml gentamycin, 100μM β-mercaptoethanol (all from Life Technologies, Carlsbad, CA) and 100 ng/ml basic fibroblast growth factor (bFGF) (PeproTech, Rocky Hill, NJ) and mechanically passaged every 2–3 d. Colonies were collected after 2–3 weeks in culture.

A single clone of CHIPS-W was expanded. From a single iPSC colony, 10 to 12 sub-colonies ($5.05 \pm 0.65 \times 10^5$ live cells) were grown in DMEM knockout media without serum replacement and bFGF on Vitonectin XF™ (Stem Cell Technologies, Vancouver, Canada) coated feeder-free plates for 24 h. Supernatant was collected, centrifuged (1200 g × 10 min) and stored (−80°C). iPSCs at passage between 12 to 14 were used in this study. Serum-free knockout media without bFGF served as cell-free control media. Conditioned media from un-induced CCD1 human foreskin fibroblasts (ATCC) served as control fibroblast CM [10].

Label-free iPSC CM protein quantification (proteomics)

Conditioned cell media were incubated twice with StrataClean™ resin slurry (room temperature × 60 min; Agilent Technologies, Basel, Switzerland), and sedimented (230 RCF × 2 min). Proteins bound to StrataClean™ beads were eluted with Lämmli buffer by boiling × 5 min. The two protein extracts were combined and the proteins separated by letting the dye front migrate only 1.5cm into a 12.5% SDS-PAGE. Proteins were stained by Coomassie

and each lane was cut into 5 horizontal slices. Each gel slice was subjected to in-gel digestion and LC-MS/MS [15] using a 40 min organic solvent gradient for peptide separation. Data were acquired using Orbitrap XL ETD (ThermoFisher, Reinach, Switzerland) and a data-dependent decision tree switching between collision-induced (CID) or electron-transfer activated peptide dissociation (ETD), triggering ETD when precursor ions had a charge state of 3+ and higher and the mass-over-charge values were <650 for 3+ ions, <900 (4+), <950 (5+), or no restriction with charges >5+, respectively. For ETD the ion time for the fluoranthene reagent accumulation was set to 120 ms at an AGC target of 3e5. Reaction time was set to 90 ms and supplemental activation was used. Parameters for CID and full MS data acquisition were described [15]. CID and ETD fragment spectra were extracted to separate peak lists and searched separately against bovine and human proteins of the SwissProt protein database release 2010_12 using the CID and ETD scoring model implemented in the Phenyx search algorithm. Protein identifications were accepted when at least 2 unique peptide sequences (at a 1% false discovery rate) were identified per protein. Peptide match score summation (PMSS) value for each identified protein was used as a semi-quantitative abundance estimate.

Hyperoxia exposure

Lung cells—Primary human AT1 cells were grown in Prigrow III medium (both from Applied Biological Materials, Richmond, BC, Canada) with 10% heat inactivated fetal bovine serum and 1% penicillin-streptomycin in extracellular matrix-coated flasks incubated at 37°C in 95% air-5% CO_2 × 12h. About 50,000 cells were seeded in six-well plates and exposed to either air or 95% O_2 with 5% CO_2 in a sealed humidified chamber (Billups-Rothenberg, Del Mar, CA) at 37°C × 24h.

Animals—Male Sprague-Dawley rats (~300g, Charles River Laboratories, Wilmington, MA) were anesthetized by intraperitoneal (i.p.) injection of ketamine (50 mg/kg) and xylazine (5mg/kg) and intubated. Heart rate and transcutaneous O_2 saturation were monitored via tail cuff (Kent Scientific, Torrington, CT). Designated media (iPSC-CM or fibroblast-CM or cell-free, 0.5ml each) was instilled into the trachea and the animal rotated side to side. Upon recovery 1 h later, animals were exposed to 90% O_2 in an environmental chamber (Biospherix™, Lacona, NY) × 3 d. Body weight was measured daily. Following exposure, animals were killed (i.p. overdose of pentobarbital 86mg/kg, and phenytoin 11mg/kg). The left lung was perfused and snap-frozen in liquid N_2. The right lung was fixed by tracheal instillation of 4% paraformaldehyde (airway pressure 25 cmH_2O). Tissue of the right caudal lobe was sampled, embedded in paraffin, sectioned (4μm thick) and stained with trichrome. Results were compared to control animals exposed to 21% O_2. Five to 7 animals per group were used.

Assays

Total antioxidant capacity—Copper reducing equivalents (CRE) were measured using a calorimetric assay (OxiSelect, Cell BioLabs, San Diego) based on reduction of copper (II) to copper (I).

Apoptosis—Caspase-8 activity was measured by colorimetric assay with detection of the chromophore p-nitroaniline (pNA) after its cleavage by caspase from labeled specific substrates (ApoAlert™, Clontech, Mountain View, CA).

Oxidative damage—*DNA damage* was measured from 8-OHdG formation. DNA was extracted, precipitated (100% ethanol), washed (70% ethanol), suspended in 8mM NaOH, and 8-OHdG measured by ELISA (OxiSelect™, Cell BioLabs, San Diego, CA). *Protein oxidation* was measured from carbonyl level (OxiSelect™, Cell BioLabs) against a reduced/oxidized bovine serum albumin (BSA) standard curve. *Lipid oxidation* was measured from 8-isoprostane level by enzyme immunoassay (Cayman Chemical, Ann Arbor, MI).

Antioxidant reporter—Dual-luciferase antioxidant reporter assay (tandem ARE's-driven firefly luciferase and constitutively expressed Renilla luciferase, Cignal, SA Biosciences, Valencia, CA) was used to measure Nrf1 and Nrf2 transcriptional activation of ARE's as the ratio of firefly-to-Renilla luciferase signal.

Quantitative Real-Time PCR

Based on proteomic analysis of iPSC secretome (Supplemental Table S1) and earlier studies [12, 16], 19 Nrf2 antioxidant genes were selected; primers (Integrated Technologies, Coralville, IA, USA) are shown in Supplemental Table S2. Total RNA was extracted from rat lung (TRIzol®, Life Technologies, USA). Complementary DNA (cDNA) was generated with oligo-dT primers (Omniscript RT kit, QIAGEN, Hilden, Germany). PCR used SYBR Green master mix (QIAGEN) on an ABI Prism 7000 Sequence Detector (Applied BioSystems, Foster City, CA) with one cycle (95 °C × 10 min) and then 40 cycles (95 °C × 15 s and 60 °C × 1 min) for each sample. Cycle threshold (Ct) values of the samples were calculated; target gene transcripts were analyzed and normalized to the Ct of 18S RNA. Relative abundance was represented by $2^{-\Delta\Delta Ct}$ with respect to the control group.

Immunoblot

Lung tissue lysates were prepared in RIPA buffer (150mM NaCl, 50mM Tris·HCl, pH 7.4, 5mM EDTA, 1% Triton X-100, 0.5% deoxycholate, and 0.1% SDS) containing fresh phosphatase and protease inhibitors, and cleared by centrifugation (14,000×g, 4°C, 30 min). 30μg of proteins per lane were fractionated by SDS-PAGE, transferred to polyvinylidene difluoride membranes, blocked with 5% nonfat milk, and incubated overnight (4°C) with primary antibodies against metallothionein A (MTA, all isoforms, Santa Cruz, Dallas, TX, sc-11377, 1:500), peroxidasin homolog (PXDN, Abcam, Cambridge, MA, ab179663, 1:500), and heme oxygenase 1 and 2 (HOX1 and HOX2, Abcam, ab13248, 1:500 and ab90492, 1:1000, respectively), followed by horseradish peroxidase-conjugated secondary antibodies. Signal was visualized by enhanced chemiluminescence (Amersham, Arlington Heights, IL), quantified by densitometry (ImageQuant, GE Healthcare Bio-Sciences, Pittsburgh, PA) and expressed as a ratio to β-action.

Immunofluorescence

To confirm pluripotency, iPSC colonies were fixed (3% paraformaldehyde × 30 min), washed with phosphate-buffered saline (PBS) and permeabilized with 0.5% Triton. After

blocking with 5% BSA, the colonies were incubated overnight with primary antibodies (OCT3/4, 1:50; NANOG, 1:50; TRA-1-60, 1:200; and TRA-1-81,1:200; all from Santa Cruz, Dallas, TX) followed by secondary antibody (anti-mouse Cy3, anti-rabbit FITC, 1:1,000). Isotype control antibodies were: anti-mouse IgG2b for Oct3/4, anti-goat IgG for Sox2 and Nanog, and anti-mouse IgM for TRA-1-60 and TRA-1-81 (all Abcam, Cambridge, UK). Images were taken using a confocal laser scanning microscope (LSM 710, Carl Zeiss, Germany).

For immunocytochemistry, 4% paraformaldehyde-fixed iPSCs were incubated with 3% donkey serum in 0.3% Triton X-100 in PBS (blocking) and exposed to rat anti-human αKlotho monoclonal antibody (1:1000, KM2076, overnight at 4°C, Trans Genic, Fukuoka, Japan), followed by incubation with secondary donkey anti-rat antibody conjugated to Alexa Fluor 555 (A31570, Invitrogen, Carlsbad, CA) at room temperature × 60min. Filamentous actin was labeled with rhodamine phalloidin (R415, Invitrogen), and nuclei with 4′,6-diamidino-2-phenylindole (DAPI, P36931, Thermo Fisher, Waltham, MA), and imaged with a laser scanning microscope (Zeiss LSM 880, Advanced Imaging Microscopy, Germany).

αKlotho immunodepletion

Frozen iPSC supernatant was thawed (37°C) and immediately placed on ice. Two aliquots of 50μl were diluted in serum-free DMEM (1:5 ratio) in low adhesion tubes. Dilution was necessary because αKlotho concentration in undiluted iPSC supernatant was too high to permit complete immunodepletion. To the diluted iPSC supernatant, 5 μg of KM2076 anti-αKlotho monoclonal antibody (TransGenics, Fukuoka, Japan) (*αKlotho depletion*), or an equal amount of non-immune control IgG2a (*negative control*), was added. A third group (fibroblast conditioned medium; CM) was also diluted 5-fold and included as a control for αKlotho-null medium. Immunoprecipitation occurred at 4°C overnight with both KM2076 and non-immune IgG. The next morning, 50μl of Protein A/G Agarose slurry (Thermo Scientific/Pierce, USA), was added to each tube (rocked 4 h at 4°C). Samples were spun (6000 g × 1 min), and the supernatants were collected and stored at 4°C for experiments. Following immunodepletion, αKlotho content was checked by immunoblots (rat anti-human αKlotho KM2076, 1:10,000). The αKlotho-immunodepleted iPSC CM (1:5 dilution) or IgG control undepleted CM (1:5 dilution), or undiluted undepleted CM, was added to cultured AT1 cells followed by hyperoxia exposure (95% O_2 × 24 h). Triplicate experiments were performed.

αKlotho standards

Conditioned media containing αKlotho were prepared as described [12]. Chinese hamster ovary (CHO) cells were stably transfected with soluble αKlotho cDNA or empty vector. Serum-free DMEM was added 16h post-transfection and again after another 16h; the supernatant containing recombinant soluble αKlotho along with other secreted proteins were collected and stored (−80°C). As current commercial assays of αKlotho yield inconsistent results, we quantified αKlotho concentration by an immunoprecipitation-immunoblot method with a specific synthetic antibody (sb106 Fab) that recognizes human, rat, and mouse αKlotho in its native form [17].

Statistics

Results from 5–7 animals per group, duplicate immunoblots, and triplicate independent assays or *in vitro* experiments, expressed as mean±SD, were analyzed by factorial or repeated measures ANOVA with post-hoc Fisher's Protected Least Significant Difference test (Statview v5.0, SAS Institute, Cary, NC). $P<0.05$ was considered significant.

Results

iPSC colonies were generated from adult human foreskin fibroblasts [10, 14], characterized by positive pluripotency markers OCT3/4, NANOG, TRA-1-60 and TRA-1-81 (Fig. 1A). No signal was detected when cells were stained with Isotype antibodies. iPSCs express abundant αKlotho (Fig. 1B) including full length (540–1,500 pM) and KL1 (~600 pM) and KL2 fragments (~300 pM) whereas typical αKlotho concentration in normal human and rat serum is 20–60 pM [16, 17]. Although there are batch-to-batch variations, all batches of iPSC secretome exhibit highly elevated αKlotho concentration.

In vitro cytoprotection

Addition of iPSC-conditioned media (CM) to human alveolar type-1 (AT1) cells cultured in normoxia (21% O_2) had little effect compared to control media (fibroblast CM, or cell-free serum-free media); however, iPSC CM attenuated hyperoxia (95% O_2)-induced oxidative damage to DNA (8-hydroxy-2′-deoxyguanosine, 8-OHdG, Fig. 2A), lipid (8-isoprostane, Fig. 2B) and protein (carbonyl, Fig. 2C). iPSC CM mitigated hyperoxia-induced depletion of endogenous total antioxidant capacity (TAC) measured by copper-reducing equivalents (CRE, Fig. 2D), and is associated with significant upregulation of Nrf2 ARE reporter activity (Fig. 2E).

In vivo lung protection

Adult rats received iPSC CM, fibroblast CM or cell-free media (0.5mL) via tracheal instillation followed by hyperoxia exposure (90% O_2 × 3 d) to induce diffuse lung injury [12]. Compared to treatment with control media, iPSC CM treatment attenuated cell/debris exudation into alveolar air spaces (Fig. 3A) and oxidative damage to DNA (8-OHdG, Fig. 3B), lipid (8-isoprostane, Fig. 3C) and protein (carbonyl, Fig. 3D), reduced apoptosis (caspase activity, Fig. 3E) and the upregulation of endogenous TAC (Fig. 3F). Lungs from rats treated with iPSC CM showed elevated mRNA expression of Nrf2 target antioxidant genes (Fig. 4A). Protein products of two genes – Metallothionein (MTA) and peroxidasin (PXDN) – were examined by immunoblot and were significantly elevated in iPSC CM-treated lungs (Fig. 4B).

Role of αKlotho

The high αKlotho content in undiluted iPSC CM precludes complete depletion. We diluted iPSC CM (1:5) and then immunodepleted αKlotho using anti-αKlotho IgG antibody (Fig. 5A). αKlotho-depleted 1:5 diluted iPSC CM was added to AT1 cells exposed to 95% O_2 and compared to addition of 1:5 diluted mock-immunodepleted, or undepleted diluted iPSC CM. Removal of αKlotho impaired the protection by iPSC CM against hyperoxic DNA damage (8-OHdG, Fig. 5B) and cell injury (lactate dehydrogenase, LDH, release, Fig. 5C), and

reduced the expected iPSC CM-mediated increase in endogenous TAC (CRE, Fig. 5D). Control 1:5 diluted CM was subjected to the same depletion procedure using non-immune IgG instead of anti-αKlotho so the loss of cytoprotection in αKlotho-depleted iPSC CM was not due to procedure-related non-specific inactivation.

Discussion

Summary

This is the first report that cell-free iPSC secretome confers antioxidative cytoprotection *in vitro* and *in vivo* in part via activation of Nrf2 network of antioxidant proteins, and the first to identify a source of the Nrf2 activation via abundant iPSC production of αKlotho, which explains about half of secretome-mediated cytoprotective effects and likely plays a fundamental role in iPSC maintenance.

Potential of stem cells and their products

Human stem cells derived from diverse sources can alleviate tissue injury and enhance repair and recovery. In the lung, human mesenchymal/stromal cells (MSCs) alleviate acute inflammation caused by lipopolysaccharide [18] and bacterial infection [19, 20], ameliorate ventilator-induced lung injury [21], and facilitate alveolar fluid clearance [22]. Intravenous MSC delivery is safe in acute respiratory distress syndrome [23], although efficacy, outcome, quantity of production, and potency standardization remain unclear. Circulating bone marrow-derived endothelial progenitor cells release anti-inflammatory and angiogenic factors to stimulate capillary repair and re-growth [24] and improve survival in acute lung injury [25]. Pluripotent embryonic stem cells protect against endotoxin- and bleomycin-induced lung injury [26, 27]. Advantages of iPSCs include their derivation from fully differentiated adult human cells without ethical concerns, ability to differentiate into functional lung cells [28], and be produced in large quantities for personalized therapy [29]. Delivery of iPSCs reduces lung injury due to bleomycin [5] and mesenteric ischemia-reperfusion [4]. Translational obstacles to the delivery of all types of stem cells include a low rate of cell engraftment and differentiation particularly in the lung [30–32], age-related loss of potency [33], and risks of immunogenicity and tumorigenicity [7–9, 34, 35]. These obstacles seriously impede progress in the field. In contrast, cell-free iPSC secretome can potentially avoid or minimize the adverse effects associated with intact cells. Limited available preclinical studies show that iPSC secretome facilitates alveolar epithelial repair *in vitro* and mitigates bleomycin lung injury *in vivo* [10]. Two of the many components of iPSC secretome, hepatocyte growth factor (HGF) [10] and interferon-γ induced protein-10 [5, 11], reportedly exert anti-fibrotic actions in the lung partly by inhibiting NF-kB/NKRF [36] and PI3K/Akt [11] pathways.

αKlotho in iPSC secretome

The role of αKlotho in iPSCs has not been described. αKlotho is a single-pass transmembrane protein most highly expressed in the kidney [37], and also in brain, heart, parathyroid gland [37], breast [38], and gonads [39]. Lung parenchyma has little endogenous αKlotho expression [12, 16, 40, 41]. αKlotho protein expression is reported in human bronchial epithelia [42] and mRNA expression in human alveolar macrophages [43].

Transmembrane αKlotho is a co-receptor for fibroblast growth factor FGF-23 in mineral regulation [37]. The extracellular domain of αKlotho is cleaved by secretases and circulates to distant organs [37]. Circulating αKlotho derives mainly from the kidney [44]. Enrichment of αKlotho in iPSC secretome may result from demethylation of the αKlotho promoter and transcriptional activation [45, 46].

αKlotho is an essential cell maintenance factor. Homozygous hypomorphic mice without circulating αKlotho are small and develop widespread premature organ degeneration and death by 9–12 weeks of age [41]. Heterozygous hypomorphic mice (50% of normal serum αKlotho level) are normal at baseline except the lung exhibits age-related air space enlargement and oxidative damage [12]. Circulating αKlotho readily exits alveolar capillaries to directly access the epithelium and protects against insults [16, 40]. Exogenous αKlotho alleviates hyperoxic and phosphotoxic damage to human AT1 cells *in vitro*, hyperoxic damage to rat lungs *in vivo* [12], and the acute lung damage associated with serum αKlotho deficiency due to acute kidney injury in rats [16]. Pleiotropic αKlotho actions include anti-oxidation [47, 48], anti-phosphotoxicity [49], anti-apoptosis [12], anti-fibrosis [50] and induction of endothelial nitric oxide production [51]. Circulating αKlotho modulates growth factor signaling pathways including insulin/IGF-1 [52], Wnt [53], CYP11B2, erythropoietin receptor, and ion channels activities [47, 54, 55]. αKlotho is also an anti-oxidant that induces manganese superoxide dismutase [48] and upregulates an array of Nrf2-related antioxidant proteins [12, 16]. In addition, αKlotho acts as a tumor suppressor [38, 56, 57] and an inhibitor of progenitor cell senescence [47, 58–60], and is essential for normal proliferation and differentiation of adipose-derived stem cells [61]. In this study, the highly enriched αKlotho content in iPSC secretome strongly suggest that αKlotho plays a fundamental role in stem cell maintenance. The antioxidative protection conferred by αKlotho in the iPSC CM is consistent with that observed following systemic delivery of exogenous αKlotho in lung injury caused by hyperoxia or as a complication of acute kidney injury [12, 16].

Critique of methods and study limitations

Despite inevitable batch-to-batch variations, αKlotho concentration in iPSC secretome is consistently elevated five to more than ten-fold above normal serum concentration in all batches. Lung injury and αKlotho biology are well-characterized in the Sprague-Dawley rat model [12, 16, 62], as is the ability for αKlotho to confer cytoprotection in many organs [37]. Residual αKlotho may remain even in the diluted immunodepleted iPSC CM. However, based on the sensitivity of our monoclonal antibody and the minimum amount of αKlotho that can be detected by immunoprecipitation-immunoblot, the highest residual αKlotho concentration that could have remained in the iPSC CM after immunodepletion is 2–5 pM. We have never observed, nor has any other laboratory reported, any cytoprotection by αKlotho using any mechanism at concentrations less than 20–50 pM. The complex composition of iPSC secretome and interactions among its components require further elucidation; here we focused on antioxidation via one highly enriched factor. Additional factors in the secretome yet to be identified could contribute to the residual cytoprotection not accounted for by αKlotho. Mechanisms of αKlotho action other than antioxidation may also play a role. Besides its independent actions, αKlotho may interact with other

secretome-derived or endogenous factors and pathways to modulate outcome. There may be interspecies difference between the human origin of secretome and the rat model. Efficacy of iPSC secretome against repetitive or chronic injury has not been addressed. Our data offer proof-of-principle support for translational development of cell-free targeted delivery of iPSC products; however, the safety profile of long-term secretome administration remain to be defined.

Conclusions

iPSCs produce abundant αKlotho, a potent cell maintenance and antioxidative factor, and an activator of the Nrf2 network that increases endogenous antioxidants to mitigate oxidative stress damage. Although the iPSC secretome undoubtedly contains multiple cytoprotective proteins, we show here that the marked enrichment of αKlotho could explain approximately half of the antioxidative effects of the secretome on lung cells and whole lungs. These results establish the feasibility, efficacy and mechanistic basis of targeted delivery of cell-free iPSC secretome, and support the translational potential of delivering cell-free stem cell-based therapy for protection from lung injury without incurring many of the drawbacks associated with delivery of intact stem cells. This approach may also be applicable to injury protection in other organs.

Supplementary Material

Refer to Web version on PubMed Central for supplementary material.

Acknowledgments

We thank the staff of the Animal Resources Center at UT Southwestern, Prof. Anis Feki, Ann-Barbara Tschirren, Dr. Fabian Blank, and the staff of the Microscopy Imaging Center at the University of Bern for their assistance. This research was supported by the National Heart, Lung and Blood Institute Grants R01 HL134373 and U01 HL111146 (both CCH), National Institute of Diabetes, Digestive & Kidney Diseases Grants R01-DK091392 and DK092461, Charles & Jane Pak Foundation, and O'Brien Kidney Research Center (P30-DK-07938) (all OWM), and the Swiss National Science Foundation (SNF 310030_141102) (TG). The content is solely the authors' responsibility and does not necessarily represent official views of the funding agencies.

Supported by:

National Heart, Lung and Blood Institute Grants R01 HL40070, U01 HL111146 and U01 HL110967 (all CCH), National Institute of Diabetes, Digestive & Kidney Diseases Grants R01-DK091392, R01-DK092461, and P30-DK-07938 (the O'Brien Kidney Research Center), Charles & Jane Pak Foundation (all OWM), and the Swiss National Science Foundation (SNF 310030_141102) (TG).

Concept and design, provision of study material, collection and/or assembly of data, data analysis and interpretation, manuscript writing, final approval

Provision of study material, collection and/or assembly of data, data analysis and interpretation

Provision of study material, collection and/or assembly of data, data analysis and interpretation

Provision of study material, collection and/or assembly of data, data analysis and interpretation

Provision of study material, collection and/or assembly of data, data analysis and interpretation

Provision of study material, collection and/or assembly of data, data analysis and interpretation

Concept and design, financial support, administrative support, provision of study material, collection and/or assembly of data, data analysis and interpretation, manuscript writing, final approval of manuscript

Concept and design, financial support, administrative support, provision of study material, collection and/or assembly of data, data analysis and interpretation, manuscript writing, final approval of manuscript

Concept and design, financial support, administrative support, provision of study material, collection and/or assembly of data, data analysis and interpretation, manuscript writing, final approval of manuscript

References

1. Tajiri N, Acosta SA, Shahaduzzaman M, et al. Intravenous transplants of human adipose-derived stem cell protect the brain from traumatic brain injury-induced neurodegeneration and motor and cognitive impairments: cell graft biodistribution and soluble factors in young and aged rats. J Neurosci. 2014; 34:313–326. [PubMed: 24381292]
2. Tsuji O, Miura K, Okada Y, et al. Therapeutic potential of appropriately evaluated safe-induced pluripotent stem cells for spinal cord injury. Proc Natl Acad Sci U S A. 2010; 107:12704–12709. [PubMed: 20615974]
3. Yang KY, Shih HC, How CK, et al. IV delivery of induced pluripotent stem cells attenuates endotoxin-induced acute lung injury in mice. Chest. 2011; 140:1243–1253. [PubMed: 21835903]
4. How CK, Hou SK, Chen LK, et al. Induced pluripotent stem cells alleviate lung injury from mesenteric ischemia-reperfusion. J Trauma Acute Care Surg. 2015; 79:592–601. [PubMed: 26402533]
5. How CK, Chien Y, Yang KY, et al. Induced pluripotent stem cells mediate the release of interferon gamma-induced protein 10 and alleviate bleomycin-induced lung inflammation and fibrosis. Shock. 2013; 39:261–270. [PubMed: 23364435]
6. Ohi Y, Qin H, Hong C, et al. Incomplete DNA methylation underlies a transcriptional memory of somatic cells in human iPS cells. Nat Cell Biol. 2011; 13:541–549. [PubMed: 21499256]
7. Cao J, Li X, Lu X, et al. Cells derived from iPSC can be immunogenic - yes or no? Protein Cell. 2014; 5:1–3. [PubMed: 24474200]
8. Jiang Z, Han Y, Cao X. Induced pluripotent stem cell (iPSCs) and their application in immunotherapy. Cell Mol Immunol. 2014; 11:17–24. [PubMed: 24336163]
9. Abad M, Mosteiro L, Pantoja C, et al. Reprogramming in vivo produces teratomas and iPS cells with totipotency features. Nature. 2013; 502:340–345. [PubMed: 24025773]
10. Gazdhar A, Grad I, Tamo L, et al. The secretome of induced pluripotent stem cells reduces lung fibrosis in part by hepatocyte growth factor. Stem Cell Res Ther. 2014; 5:123. [PubMed: 25384638]
11. Li LF, Liu YY, Yang CT, et al. Improvement of ventilator-induced lung injury by IPS cell-derived conditioned medium via inhibition of PI3K/Akt pathway and IP-10-dependent paracrine regulation. Biomaterials. 2013; 34:78–91. [PubMed: 23063297]
12. Ravikumar P, Ye J, Zhang J, et al. alpha-Klotho protects against oxidative damage in pulmonary epithelia. Am J Physiol Lung Cell Mol Physiol. 2014; 307:L566–575. [PubMed: 25063799]
13. Ravikumar P, Menon JU, Punnakitikashem P, et al. Nanoparticle facilitated inhalational delivery of erythropoietin receptor cDNA protects against hyperoxic lung injury. Nanomedicine. 2016; 12:811–821. [PubMed: 26518603]
14. Grad I, Hibaoui Y, Jaconi M, et al. NANOG priming before full reprogramming may generate germ cell tumours. Eur Cell Mater. 2011; 22:258–274. discussio 274. [PubMed: 22071697]
15. Al Kaabi A, Traupe T, Stutz M, et al. Cause or effect of arteriogenesis: compositional alterations of microparticles from CAD patients undergoing external counterpulsation therapy. PLoS One. 2012; 7:e46822. [PubMed: 23056467]
16. Ravikumar P, Li L, Ye J, et al. alphaKlotho deficiency in acute kidney injury contributes to lung damage. J Appl Physiol (1985). 2016; 120:723–732. [PubMed: 26718784]
17. Barker SL, Pastor J, Carranza D, et al. The demonstration of alphaKlotho deficiency in human chronic kidney disease with a novel synthetic antibody. Nephrol Dial Transplant. 2015; 30:223–233. [PubMed: 25324355]
18. Rojas M, Cardenes N, Kocyildirim E, et al. Human adult bone marrow-derived stem cells decrease severity of lipopolysaccharide-induced acute respiratory distress syndrome in sheep. Stem Cell Res Ther. 2014; 5:42. [PubMed: 24670268]

19. Asmussen S, Ito H, Traber DL, et al. Human mesenchymal stem cells reduce the severity of acute lung injury in a sheep model of bacterial pneumonia. Thorax. 2014; 69:819–825. [PubMed: 24891325]
20. Devaney J, Horie S, Masterson C, et al. Human mesenchymal stromal cells decrease the severity of acute lung injury induced by E. coli in the rat. Thorax. 2015; 70:625–635. [PubMed: 25986435]
21. Hayes M, Masterson C, Devaney J, et al. Therapeutic efficacy of human mesenchymal stromal cells in the repair of established ventilator-induced lung injury in the rat. Anesthesiology. 2015; 122:363–373. [PubMed: 25490744]
22. McAuley DF, Curley GF, Hamid UI, et al. Clinical grade allogeneic human mesenchymal stem cells restore alveolar fluid clearance in human lungs rejected for transplantation. Am J Physiol Lung Cell Mol Physiol. 2014; 306:L809–815. [PubMed: 24532289]
23. Wilson JG, Liu KD, Zhuo H, et al. Mesenchymal stem (stromal) cells for treatment of ARDS: a phase 1 clinical trial. Lancet Respir Med. 2015; 3:24–32. [PubMed: 25529339]
24. Baker CD, Seedorf GJ, Wisniewski BL, et al. Endothelial colony-forming cell conditioned media promote angiogenesis in vitro and prevent pulmonary hypertension in experimental bronchopulmonary dysplasia. Am J Physiol Lung Cell Mol Physiol. 2013; 305:L73–81. [PubMed: 23666751]
25. Burnham EL, Taylor WR, Quyyumi AA, et al. Increased circulating endothelial progenitor cells are associated with survival in acute lung injury. Am J Respir Crit Care Med. 2005; 172:854–860. [PubMed: 15976374]
26. Hao Q, Zhu YG, Monsel A, et al. Study of Bone Marrow and Embryonic Stem Cell-Derived Human Mesenchymal Stem Cells for Treatment of Escherichia coli Endotoxin-Induced Acute Lung Injury in Mice. Stem Cells Transl Med. 2015; 4:832–840. [PubMed: 25999518]
27. Wang YY, Li XZ, Wang LB. Therapeutic implications of mesenchymal stem cells in acute lung injury/acute respiratory distress syndrome. Stem Cell Res Ther. 2013; 4:45. [PubMed: 23673003]
28. Huang SX, Islam MN, O'Neill J, et al. Efficient generation of lung and airway epithelial cells from human pluripotent stem cells. Nat Biotechnol. 2014; 32:84–91. [PubMed: 24291815]
29. Hawkins F, Kotton DN. Embryonic and induced pluripotent stem cells for lung regeneration. Ann Am Thorac Soc. 2015; 12(Suppl 1):S50–53. [PubMed: 25830836]
30. Ortiz LA, Gambelli F, McBride C, et al. Mesenchymal stem cell engraftment in lung is enhanced in response to bleomycin exposure and ameliorates its fibrotic effects. Proc Natl Acad Sci U S A. 2003; 100:8407–8411. [PubMed: 12815096]
31. Martinez-Gonzalez I, Moreno R, Petriz J, et al. Engraftment potential of adipose tissue-derived human mesenchymal stem cells after transplantation in the fetal rabbit. Stem Cells Dev. 2012; 21:3270–3277. [PubMed: 22738094]
32. Cai SX, Liu AR, Chen S, et al. The Orphan Receptor Tyrosine Kinase ROR2 Facilitates MSCs to Repair Lung Injury in ARDS Animal Model. Cell Transplant. 2016; 25:1561–1574. [PubMed: 26531175]
33. Bustos ML, Huleihel L, Kapetanaki MG, et al. Aging mesenchymal stem cells fail to protect because of impaired migration and antiinflammatory response. Am J Respir Crit Care Med. 2014; 189:787–798. [PubMed: 24559482]
34. Zhao T, Zhang ZN, Westenskow PD, et al. Humanized Mice Reveal Differential Immunogenicity of Cells Derived from Autologous Induced Pluripotent Stem Cells. Cell Stem Cell. 2015; 17:353–359. [PubMed: 26299572]
35. Griscelli F, Feraud O, Oudrhiri N, et al. Malignant germ cell-like tumors, expressing Ki-1 antigen (CD30), are revealed during in vivo differentiation of partially reprogrammed human-induced pluripotent stem cells. Am J Pathol. 2012; 180:2084–2096. [PubMed: 22425713]
36. Liu YY, Li LF, Yang CT, et al. Suppressing NF-kappaB and NKRF Pathways by Induced Pluripotent Stem Cell Therapy in Mice with Ventilator-Induced Lung Injury. PLoS One. 2013; 8:e66760. [PubMed: 23840526]
37. Hu MC, Kuro-o M, Moe OW. Renal and extrarenal actions of Klotho. Semin Nephrol. 2013; 33:118–129. [PubMed: 23465499]
38. Wolf I, Levanon-Cohen S, Bose S, et al. Klotho: a tumor suppressor and a modulator of the IGF-1 and FGF pathways in human breast cancer. Oncogene. 2008; 27:7094–7105. [PubMed: 18762812]

39. Li SA, Watanabe M, Yamada H, et al. Immunohistochemical localization of Klotho protein in brain, kidney, and reproductive organs of mice. Cell Struct Funct. 2004; 29:91–99. [PubMed: 15665504]
40. Hsia CC, Ravikumar P, Ye J. Acute lung injury complicating acute kidney injury: A model of endogenous alphaKlotho deficiency and distant organ dysfunction. Bone. 2017 In press.
41. Kuro-o M, Matsumura Y, Aizawa H, et al. Mutation of the mouse klotho gene leads to a syndrome resembling ageing. Nature. 1997; 390:45–51. [PubMed: 9363890]
42. Gao W, Yuan C, Zhang J, et al. Klotho expression is reduced in COPD airway epithelial cells: effects on inflammation and oxidant injury. Clin Sci (Lond). 2015; 129:1011–1023. [PubMed: 26201096]
43. Li L, Wang Y, Gao W, et al. Klotho Reduction in Alveolar Macrophages Contributes to Cigarette Smoke Extract-induced Inflammation in Chronic Obstructive Pulmonary Disease. J Biol Chem. 2015; 290:27890–27900. [PubMed: 26385922]
44. Hu MC, Shi M, Zhang J, et al. Renal Production, Uptake, and Handling of Circulating alphaKlotho. J Am Soc Nephrol. 2015; 27:79–90. [PubMed: 25977312]
45. Young GH, Wu VC. KLOTHO methylation is linked to uremic toxins and chronic kidney disease. Kidney Int. 2012; 81:611–612. [PubMed: 22419041]
46. Azuma M, Koyama D, Kikuchi J, et al. Promoter methylation confers kidney-specific expression of the Klotho gene. FASEB J. 2012; 26:4264–4274. [PubMed: 22782974]
47. Kuro-o M. Klotho as a regulator of oxidative stress and senescence. Biol Chem. 2008; 389:233–241. [PubMed: 18177265]
48. Yamamoto M, Clark JD, Pastor JV, et al. Regulation of oxidative stress by the anti-aging hormone klotho. J Biol Chem. 2005; 280:38029–38034. [PubMed: 16186101]
49. Kuro-o M. A potential link between phosphate and aging–lessons from Klotho-deficient mice. Mech Ageing Dev. 2010; 131:270–275. [PubMed: 20197072]
50. Shin IS, Shin HK, Kim JC, et al. Role of Klotho, an antiaging protein, in pulmonary fibrosis. Arch Toxicol. 2015; 89:785–795. [PubMed: 24894433]
51. Saito Y, Nakamura T, Ohyama Y, et al. In vivo klotho gene delivery protects against endothelial dysfunction in multiple risk factor syndrome. Biochem Biophys Res Commun. 2000; 276:767–772. [PubMed: 11027545]
52. Bartke A. Long-lived Klotho mice: new insights into the roles of IGF-1 and insulin in aging. Trends Endocrinol Metab. 2006; 17:33–35. [PubMed: 16458526]
53. Liu H, Fergusson MM, Castilho RM, et al. Augmented Wnt signaling in a mammalian model of accelerated aging. Science. 2007; 317:803–806. [PubMed: 17690294]
54. Zhou X, Chen K, Wang Y, et al. Antiaging Gene Klotho Regulates Adrenal CYP11B2 Expression and Aldosterone Synthesis. J Am Soc Nephrol. 2016; 27:1765–1776. [PubMed: 26471128]
55. Hu MC, Shi M, Cho HJ, et al. The erythropoietin receptor is a downstream effector of Klotho-induced cytoprotection. Kidney International. 2013; 84:468–481. [PubMed: 23636173]
56. Chen B, Ma X, Liu S, et al. Inhibition of lung cancer cells growth, motility and induction of apoptosis by Klotho, a novel secreted Wnt antagonist, in a dose-dependent manner. Cancer Biol Ther. 2012; 13:1221–1228. [PubMed: 22922788]
57. Poh W, Wong W, Ong H, et al. Klotho-beta overexpression as a novel target for suppressing proliferation and fibroblast growth factor receptor-4 signaling in hepatocellular carcinoma. Mol Cancer. 2012; 11:14. [PubMed: 22439738]
58. Zhou Z, Hu CP, Wang CJ, et al. Calcitonin gene-related peptide inhibits angiotensin II-induced endothelial progenitor cells senescence through up-regulation of klotho expression. Atherosclerosis. 2010; 213:92–101. [PubMed: 20832068]
59. Vadakke Madathil S, Coe LM, Casu C, et al. Klotho deficiency disrupts hematopoietic stem cell development and erythropoiesis. Am J Pathol. 2014; 184:827–841. [PubMed: 24412515]
60. Bian A, Neyra JA, Zhan M, et al. Klotho, stem cells, and aging. Clin Interv Aging. 2015; 10:1233–1243. [PubMed: 26346243]
61. Fan J, Sun Z. The Antiaging Gene Klotho Regulates Proliferation and Differentiation of Adipose-Derived Stem Cells. Stem Cells. 2016; 34:1615–1625. [PubMed: 26865060]

62. Hu MC, Shi M, Zhang J, et al. Klotho deficiency is an early biomarker of renal ischemia-reperfusion injury and its replacement is protective. Kidney Int. 2010; 78:1240–1251. [PubMed: 20861825]

Significance

The mechanisms by which human induced pluripotent stem cells protect against tissue injury remain unclear and administration of intact cells faces many hurdles with limited success to date. We found that secretory products of these stem cells are highly enriched in an essential factor (alpha-Klotho) that activates innate antioxidant pathways to mitigate acute lung injury. Alpha-Klotho accounts for a major portion of stem cell-mediated protection in cell cultures and intact animal lungs. This novel mechanism of stem cell action provides strong rationale for translational use of stem cell secretory products in tissue protection that may overcome many of the obstacles associated with delivery of intact cells, with broad applications for alleviating injury in lungs and other organs.

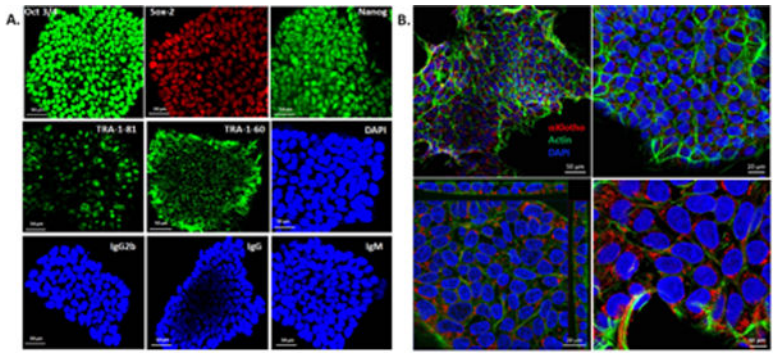

Figure 1.

A. Immunophenotypic profile of iPSC colonies. Following viral transfection of fibroblasts and culture × 2 to 3 weeks, iPSC colonies stained positive for pluripotency markers OCT3/4, Sox-2, NANOG, TRA-1-60 and TRA-1-81. DAPI stains the nuclei. The colonies were also stained for isotype control antibodies IgG2b (Oct3/4), IgG (Sox-2 and Nanog), and IgM (TRA-1-81 and TRA-1-60). Bar=50μm. ***B***. iPSC colonies imaged at different magnifications (***upper 2 panels***) show abundant expression of αKlotho (red), counterstained for filamentous actin (Alexa Fluor 488 phalloidin, green) and nuclei (DAPI, blue) Bar = 50 μm (left) and 20 μm (right). Z-section (***left lower panel***) shows the cuboidal nature of cells and further magnified (***right lower panel***) to show αKlotho in the cytoplasm. Bar = 20 μm (left) and 10 μm (right).

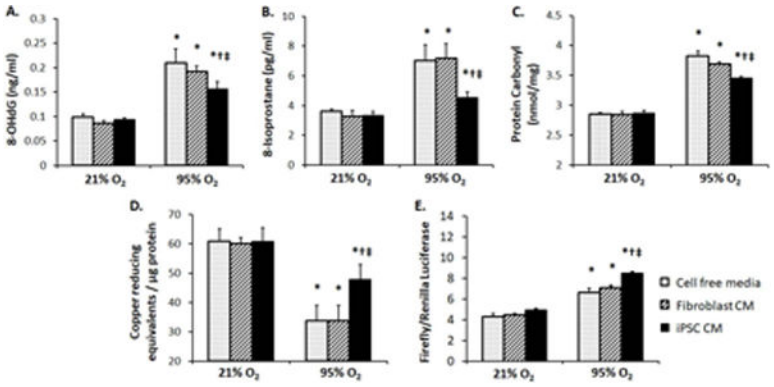

Figure 2. In vitro

effects of iPSC conditioned media (CM). Human AT1 cells were exposed to cell free media (stippled bars), fibroblast CM (hatched bars), or iPSC CM (solid black bars) in 21% or 95% O_2 × 24 h. Oxidative damage to DNA (8-OHdG, ***A***), lipid (8-isoprostane, ***B***) and protein (carbonyl, ***C***), and total antioxidant capacity (copper reducing equivalents, ***D***) and Nrf2 ARE antioxidant reporter activation (firefly/renilla luciferase, ***E***) were measured in triplicates. Mean±SD. P≤0.05 by ANOVA: * vs. 21% O_2 at the same conditions; † vs. cell free media at the same O_2 level; ‡ vs. fibroblast CM at the same O_2 level.

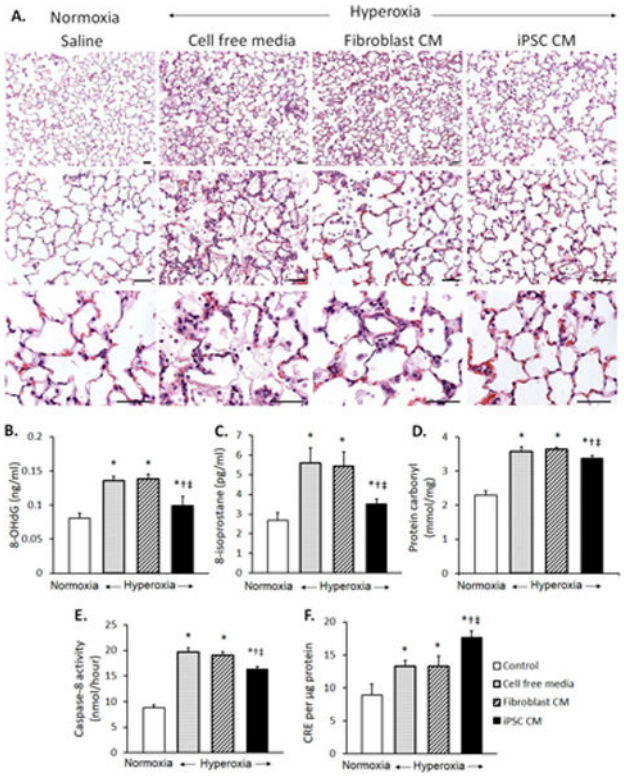

Figure 3.

A. Distal lung morphology in rats receiving tracheal instillation of iPSC conditioned media (CM), fibroblast CM, or cell free media, followed by 90% O_2 exposure × 3 d (hyperoxia), compared to control animals instilled with saline and exposed to 21% O_2 (normoxia). Hematoxylin-eosin stain. Bar = 50µm. ***B–F***. *In vivo* effects of cell free media (stippled bars), fibroblast CM (hatched bars), or iPSC CM (solid black bars) on oxidative damage to DNA (8-OHdG, ***B***), lipid (8-isoprostane, ***C***) and protein (carbonyl, ***D***), and apoptosis (caspase-8 activity, ***E***) and total antioxidant capacity (copper reducing equivalent, CRE, ***F***), in lung tissue from rats exposed to hyperoxia were compared to control lungs of animals exposed to normoxia (open bars). Triplicate assays were performed. Mean±SD; 5–7 animals per group. $p \leq 0.05$ by ANOVA: * vs. normoxia; † vs. cell free media; ‡ vs. Fibroblast CM.

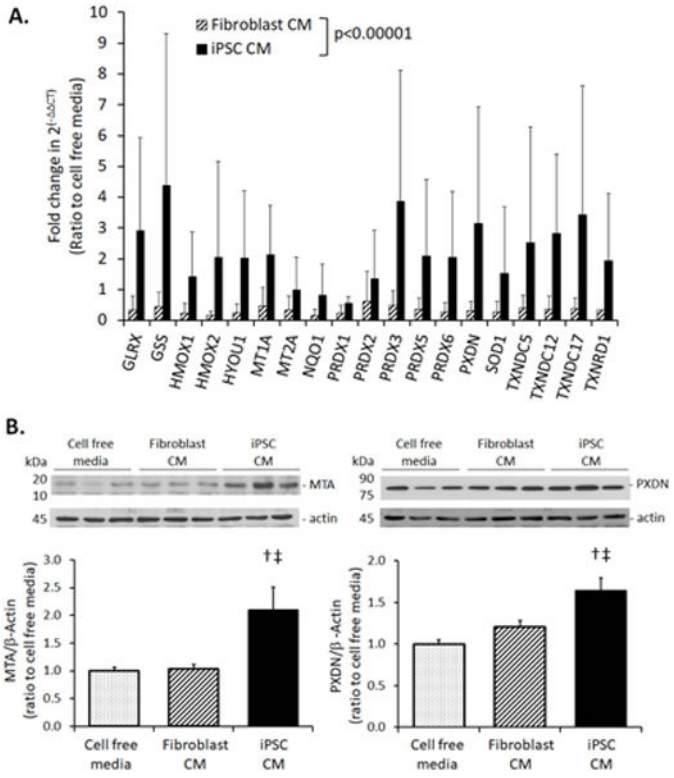

Figure 4.

A. mRNA expression of selected Nrf2 target genes measured by qPCR in the lungs of rats treated with iPSC CM (dark solid bars), fibroblast CM (hatched bars), or cell free media (set as 1.0) and exposed to 90% O_2 × 3 d. The mRNA quantity, $2^{(-\Delta\Delta CT)}$, was expressed as a ratio to the average value in control animals treated with cell free media. Gene names are shown in Supplemental Table 2. Mean±SD; 5–7 animals per group. P<0.0001, iPSC vs. fibroblast CM across all parameters by repeated measures ANOVA. ***B.*** Immunoblot of Nrf2 target proteins: metallothionein A (MTA, left) and peroxidasin (PXDN, right), in lungs of rats treated with iPSC CM (dark solid bars), fibroblast CM (hatched bars), or cell free CM (stippled bars), and exposed to 90% O_2 × 3d. Representative blots are shown (*top*). Quantitative protein expression normalized to β-actin loading are shown as ratios to the average values in control animals instilled with cell free media (=1.0) (*bottom*). Mean±SD. Duplicate assays; 5–7 animals per group. P<0.05: † vs. cell free media; ‡ vs. fibroblast CM; factorial ANOVA.

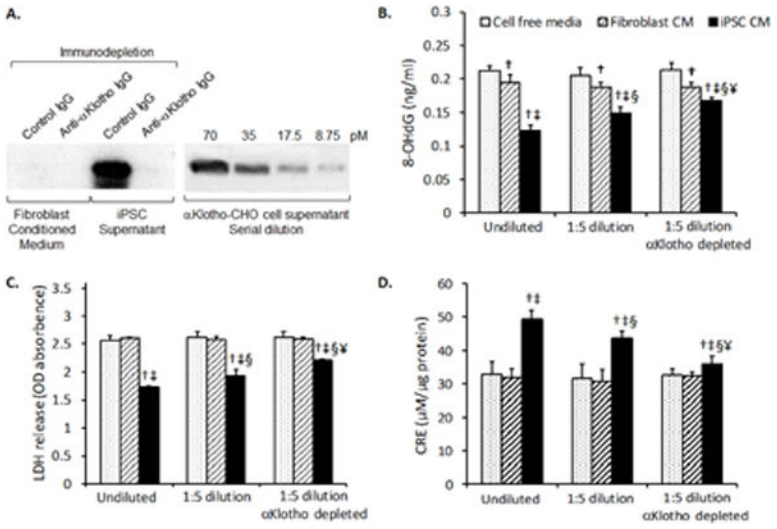

Figure 5.

A. Immunodepletion of αKlotho from iPSC supernatant. ***Left panel:*** Fibroblast conditioned media and iPSC supernatant were diluted 5-fold with serum-free DMEM media and incubated with either anti-αKlotho IgG (immunodepletion) or control IgG (mock depletion) overnight. Protein A/G agarose was used to capture the immunocomplexes, which were released from the agarose beads with the same volume as before immunodepletion. Aliquots of media were immunoblotted for αKlotho. ***Right panel:*** αKlotho-expressing Chinese Hamster Ovary (CHO) cell supernatant with a known concentration of αKlotho (70 pM) was serially diluted and loaded onto adjacent lanes on the same gel for comparison. ***B–D.*** Cell-free media (stippled bars), untransfected fibroblast conditioned media (CM) (hatched bars), and iPSC conditioned CM (solid black bars) were added to AT1 cells as undiluted undepleted (x-axis; undiluted), diluted followed by mock-depletion (x-axis 1:5 dilution), or diluted and immunodepleted (x-axis; 1:5 dilution αKlotho depleted). Treated AT1 cells were exposed to 95% O_2 × 24 h. αKlotho-depleted iPSC CM (1:5 dilution) exhibited diminished ability to alleviate hyperoxic DNA damage (8-OHdG, ***B***) and cell damage (LDH release, ***C***) and to increase total antioxidant capacity (copper reducing equivalents, CRE, ***D***). Mean±SD; triplicate experiments. P≤0.05: † vs. cell free media, ‡ vs. fibroblast CM, under the same conditions; § vs. undiluted undepleted media; ¥ vs. 1:5 diluted mock-depleted media.